DEFENSE TECHNICAL INFORMATION CENTER
a246241

(2)

DTIC
ELECTE
FEB 2 4 1992
S D
D

FINAL TECHNICAL REPORT

ONR GRANT # N00014-89-J-1635

2-10-92

INVESTIGATIONS OF THE SEAFLOOR COUPLING CHARACTERISTICS OF THE NEW ONR OBS AND RELATED QUESTIONS

Anne Trehu
College of Oceanography
Oregon State University
Corvallis, OR 97331

ABSTRACT

A series of transient tests were conducted to determine the seafloor coupling characteristics of the new ONR OBS. Seismic energy radiated from the main recording package as a result of motion of the recording package was also measured. The vertical coupling resonances of both the recording package and the sensor package are somewhat lower than those predicted by a simple model of soil-structure interaction, but are generally in agreement with the theory. The most important result of this study is that significant energy is radiated from the recording package in response to horizontal motions of the recording package. When the sensor package is 1 m from the recording package, the amplitude of the recorded signal is similar to that recorded on the recording package. In the field, this effect will result in increased noise recorded by the sensors if the recording package is disturbed by seafloor currents or biological activity. The amplitude of this signal attenuates rapidly with distance, suggesting that an improved response can be achieved by increasing the separation between the recording package and the sensors. This effect is much less severe for vertical disturbances of the recording package.

PUBLICATIONS RESULTING FROM THIS GRANT

Trehu, A., and Sutton, G., Seafloor coupling characteristics of the new ONR OBS, to be submitted to Marine Geophysical Research.

This document has been approved for public release and sale; its distribution is unlimited.

92-04215

92 2 18 148

TABLE OF CONTENTS

Accesion For

NTIS CRA&I ☑
DTIC TAB ☐
Unannounced ☐
Justification .....

By .....
Distribution /

Availability Codes

Dist	Avail and / or Special
A-1	

Statement A per telecon Dr. Randall Jacobson
ONR/Code 1125
Arlington, VA 22217-5000

NWW 2/21/92

INTRODUCTION

Achieving good instrument/seafloor coupling has been a long sought after and long elusive objective of ocean bottom seismology. The coupling is affected by several different processes, including soil-structure interaction and vibration and tilting due to water flow around the OBS. Minimizing the effect of soil/structure interaction requires minimizing the mass of the OBS while maximizing the bearing area (Sutton and others, 1981; Zelikovitz and Prothero, 1981; Tréhu, 1981, 1985a; Sutton and Duennebier, 1988), and minimizing the effect of seafloor currents requires minimizing the cross-sectional area of the OBS (Kasahara et al., 1980; Trehu, 1985b; Sutton and Duennebier, 1988). Since most of the mass and volume of an OBS is used for the power supply and recording hardware rather than for the seismometers, placing seismometers in a small package that is separated from the main recording package is potentially an attractive means of improving the coupling (eg. Duschenes et al., 1981; Trehu and Solomon, 1981). This approach has been taken for a new OBS developed for the Office of Naval Research.

Potential disadvantages of a deployed sensor package are the additional mechanical complexity of the instrument package, which increases the chances of failure, and the possibility that the recording package itself will become a source of seafloor noise. That the second possibility may be reason for concern was first suggested in the data recorded during the 1978 Lopez Island OBS intercomparison test, during which signals from transient tests on OBS's were observed on neighboring instrument packages (Sutton et al, 1981; Trehu and Solomon, 1981). In order to evaluate the second possibility, we conducted tests to measure the seismic signal generated by motion of the recording package for the new ONR OBS.

BACKGROUND

If an OBS has volume and mass, which of course it must, its presence affects the wavefield through a variety of physical processes which are generally referred to under the umbrella of "OBS coupling." In order to determine ground motion in the absence of the instrument, recorded seismograms must be corrected for these effects, which occur because the boundary conditions at the boundaries between an OBS and the surrounding media are different from those in the absence of the OBS. This applies whether the OBS is buried or sits on the seafloor, and whether the sensors are in the main instrument package or in a separate package. When a seismic wave impinges on this boundary from below, normal and tangential forces will be applied to the boundary that will excite seismic waves in the

surrounding media. This is essentially a problem of wavefield scattering due to the presence of a single scatterer. Because of reciprocity, the resulting wavefield can be studied by applying forces to the boundary by moving the OBS.

soil-structure interaction

The solution of the scattering problem on the boundary itself gives the motion of the OBS relative to the motion of the surrounding medium in the absence of the OBS. We will refer to this part of the coupling problem as soil-structure interaction. Numerous solutions to this problem for a variety of boundary conditions are available in the civil engineering literature. The simplest model is that of a rigid plate on the surface of a half-space (eg. Arnold et al., 1955; Bycroft, 1956, 1978; Hsieh, 1962; Lamer, 1969; Luco and Westman, 1971; Lysmer and Richart, 1966; Richart et al., 1970; Robertson, 1966; Wolf, 1944). These calculations have been extended to several more complicated situations, including a layered visco-elastic medium (Luco, 1974, 1976) and a flexible plate (Iguchi and Luco, 1982). These more complicated situations cannot be solved analytically and must be treated numerically. Although the results of these studies are not directly applicable to the OBS problem because the presence of the water results in somewhat different boundary conditions, they are quite useful for obtaining a qualitative, and even semi-quantitative, understanding of the the problem (Trehu, 1985a). In particular, because of the very low shear velocity of seafloor sediments, the problem scales such that an OBS is comparable to a building on land, and the non-dimensional frequency range of many of the engineering calculations is appropriate for the OBS case.

The form of the complete solution to the coupling problem is such that it can be approximated by a very simple one-dimensional mass-spring-dashpot model in which the spring and damping coefficients for each mode of motion can be considered to be independent of frequency (referred to by Trehu (1985a) as the zero-order model). In this model, the spring and damping coefficients are a function of the mass and bearing radius of the structure and of the physical properties of the sediment, especially the shear modulus. Sutton et al. (1981) and Zelikovitz and Prothero (1981) extended this simple mass-spring-dashpot model to the OBS case by adding a correction to the mass of the OBS to account for hydrodynamic effects. For the vertical mode of motion, the undamped resonant frequency is $2[\mu(1-\nu)^{-1}rm^{-1}]^{1/2}$ where μ is the shear modulus of the underlying sediment, ν is the Poisson's ratio of the sediment, r is the bearing radius of the OBS, and m is the mass of the structure, corrected for additional inertia due to hydrodynamic effects.

Damping, expressed as the ratio of damping to critical damping, is $0.85[\rho(1-\nu)^{-1}r^3m^{-1})^{1/2}$, where ρ is the density of the sediments. The mass correction for hydrodynamic effects is $\alpha\rho_w V$, where V is the volume, ρ_w is the density of water, and α is a constant that depends on the shape of the body. For a sphere, a is 0.12; for a cylinder, it is 0.6. At frequencies well below the resonant frequency, motion of the OBS follows motion of the seafloor; for frequencies above the resonant frequency, the OBS acts as a low pass filter; near the resonant frequency, motion of the OBS is amplified and the recorded signal is therefore distorted. To achieve good coupling, we want the coupling resonant frequency to be highly damped and above the frequency range of interest. This implies that we should maximize the bearing radius and minimize the mass of the OBS. Of course, many other considerations, such as the expected roughness scale of the seafloor, also affect the desired and/or practical radius and mass.

Sutton and Duennebier (1988) have argued for an optimum radius, based on an additional correction to the mass that is interpreted to represent sediment entrained with the OBS. This additional correction comes from a second order approximation to the frequency dependant spring coefficient that is only valid for non-dimensional frequency less than 1.5 and that departs rapidly from the complete solution for larger frequencies. The optimum radius is therefore a local optimum rather than a global optimum. The results of Trehu (1985a) suggest that for non-dimensional frequencies of 2-3 the resonant frequency continues to increase and is better described by the zero-order model.

The transfer function for a given OBS package and site can be determined using a transient pull test in which a float of known buoyancy is attached to an OBS by a solenoid and then released suddenly, exciting the characteristic soil-structure resonance for that site. The theory behind and practice of the tests have been described in detail by Sutton et al. (1981) and Trehu (1985a). Both vertical and horizontal responses can be excited. Alternatively, a harmonic driving force can be used to derive the transfer function.

The simple zero-order mass-spring-dash pot model is generally consistent with coupling resonances excited by vertical transient pull tests during the Lopez Island experiments (Sutton et al., 1981). Moreover, these resonances were right within the VLF frequency band for most packages. Trehu and Solomon (1981) and Trehu (1985a) conducted a series of controlled experiments in which different anchors were used with otherwise identical OBS's to further confirm the applicability of this simple model to the vertical mode of motion. An important result of these experiments was that they demonstrated that a flowerpot-type anchor that was being used at that time on a number of

OBS's was inappropriate, as predicted by the theory, and that a plate-type anchor was desired, at least for deployments on soft sediments.

reradiation of seismic energy

Another consideration that is relevant for an OBS with a deployed sensor package is radiation of seismic energy from the recording package as it moves relative to the seafloor because of coupling resonances, seafloor currents, "fish bumps," etc. Several observations indicate that this effect may be significant. For example, during the Lopez Island intercomparison test, signals were observed on OBS's from transient tests conducted on neighboring instruments with separations of several tens of meters. Moreover, signals were observed on the MIT main package from transients on the deployed package (Trehu and Solomon, 1981), which were separated by about 1 m.

This phenomenon has also been observed on land. When the Milliken Library at Cal Tech was vibrated to study its engineering properties, signals were recorded up to a distance of 6.7 miles, and the falloff of amplitude with range was approximately proportional to r^{-1} (Jennings, 1970), consistent with Rayleigh wave propagation. Moreover, Safar (1978) exploited this phenomenon of reradiation to improve the summed coupling response of an array of geophones by positioning the geophones such that the motion due to reradiated energy from neighboring geophones cancelled the motion due to the soil-structure resonance of a single geophone.

A complete theoretical study of the OBS reradiation problem has yet to be done. A few analogous studies, however, are available in the engineering literature. Luco and Westman (1971) presented equations for the far-field displacements due to motion of a rigid disk on a half space. These correspond essentially to Rayleigh waves excited by the force exerted on the half-space by the rigid disk. For the far-field half-space solution, the frequency content of the reradiated Rayleigh waves is a function of the dimensions of the disk and the shear wave velocity in the half-space. Based on the excitation functions calculated by Luco and Westman (1971), we expect significant excitation of Rayleigh waves for frequencies lower than about 20 Hz, assuming a shear velocity of 30 m/s and a radius of 0.5 m (i.e., a typical plate-mounted instrument package on soft sediment). For instruments with several small foot pads, the high frequency cut-off will be higher, but interference effects will be set up among the waves radiated from the several foot pads.

It has been suggested that reradiation should not be a significant problem when incident wavelengths are much greater than the diameter of the baseplate. This is true for the reradiation

resulting from soil-structure interaction, which will not be strongly excited by long period incident waves. However, the potential problem of seismic energy generated from current or biologically induced motions of the recording package remains.

THE NEW ONR OBS

The new ONR OBS has been described by Sauter et al., (1990) and Jacobson et al. (1991). The main recording package, power supply, and buoyancy are housed in the main package (figure 1), which has approximate dimensions of about 1.75 m by 1 m by 1 m and weighs 694 kg on deployment, including an expendable 156 kg rectangular steel plate as an anchor. Geophones with a natural frequency of 1 Hz are housed in a sphere that is attached to the main recording package as shown in figure 1. The sensor package is attached to the main package during deployment by a mechanical arm. After the instrument reaches the seafloor, the arm releases and the sensor package is placed approximately 1 m from the main packages. After deploying the sensor package, the arm retracts, effectively decoupling the sensor package from the recording package. An additional 3 channels of data are available for recording additional sensors such as a long period pressure sensor and environmental data. In order to record the motion of the main recording package during this experiment, a second sensor package containing three orthogonal 2 Hz geophones was strapped to the frame of the recording package during this experiment, and all six channels of data were recorded simultaneously.

EXPERIMENTAL PROCEDURES

The experimental procedure we used to measure soil-structure interaction and reradiation of energy was modeled after that used to measure the soil-structure interaction of a variety of different OBS configurations during the Lopez Island Intercomparison Experiment (Sutton et al., 1981). To measure the natural soil-strucure resonance of both main and deployed package at the experiment site, divers attached calibrated weights to the packages by means of a metal plunger that was inserted into a solenoid attached to the package being tested. The weights were then released instantaneously by cutting the current to the solenoid. Attaching the floats to the instrument effectively stretches the spring of the OBS-sediment system by an amount $x_o = F_b k_o^{-1}$, where F_b is the buoyancy of the float and k_o is the static spring constant of the system. When the float is released, the response is measured as the instrument oscillates about its equilibrium position. Horizontal transients that simulate a shear wave impinging on the package can be conducted by

clamping the solenoid to the base of the package and running the line attaching the floats to the plunger through a pulley placed on the seafloor. This experimental configuration is illustrated in figure 1.

To test whether small motions of the recording package were a source of noise recorded on the deployed geophone package, the pull tests on the recording package were recorded on the sensor package as the sensor package was moved from 1 m to 6 m away from the recording package along a line parallel to the long axis of the main recording package (defined as the radial direction in subsequent discussion; see figure 1). Distances were measured by divers using a pre-marked line and represent the distance from the edge of the anchor to the edge of the anchor of the recording package. Vertical, radial and tangential transient tests were performed on the main package at each distance and recorded on both the sensor package and on the 2 Hz sensors strapped to the recording package.

Tests were conducted in Buzzards Bay, MA, at a site where similar tests had been conducted on the USGS OBS to determine the coupling parameters of various anchor configurations (Trehu, 1985a). We chose this site because the physical properties and local basement structure had been determined as part of the earlier experiment. A complete summary of the tests performed is documented in Appendix A.

DATA PROCESSING

All data were converted from the Serial Digital Data format recorded in the instruments, which includes dynamic gain ranging, to both SEGY and Lamont-AH format for further processing. Raw data traces are shown in Appendix B.

Several problems were encountered during this experiment because design and testing of the instruments had not yet been completed when the experiment was staged. One of the problems was that the maximum sample rate we could record was 128 samples/s and was not adequate to characterize the high frequency signal from the pull tests. A second problem is that the signal from several of the geophones were contaminated by an unidentified resonances; a high gain was used to boost the signal relative to this resonance, resulting in a decrease in effective dynamic range. The most serious problem was that the data that were acquired contain many spikes and other distortions of the waveform such as DC offsets (see unprocessed data in Appendix B).

To remove spikes from the data, we developed the following algorithm based on a 5-point moving window. We first calculate ADIFF1 = (abs(x[j-2] - x[j-1]) + abs(x[j+1] - x[j+2]) / 2 and ADIFF2 = (abs(x[j-1] - x[j]) + abs(x[j] - x[j+1]) / 2. If ADIFF2 > FAC*ADIFF1, where FAC

is a tolerance factor set by the user, then x[j] is considered to be a spurious spike and it is replaced by x[j]new = (x[j+1] -x[j-1]) / 2. Figure 2 compares unprocessed data to data processed with FAC = 10 and FAC = 5. For these data, FAC = 5 generally removed most of the isolated spikes. When several spikes occur together, the despiking algorithm does not modify the data; in these cases, it is indeed difficult to separate spikes from high frequency signal.

The time of the transient was determined from the in-line component recorded on the package to which the transient had been applied. This time was then entered into the trace header and defined as the event time in order to align all traces to a common relative time base.

To examine the energy radiated from the main package, traces recorded on the sensor package from pulls on the main package while the sensor package was at increasing offsets from the recording package were resorted into record sections. Implicit in this procedure is the assumption that the signal from the transients is repeatable. During transient tests on the USGS OBS (Trehu, 1985a), this assumption was confirmed through many identical transients. Moreover, the soil-structure interaction response appeared to be independent of the force applied for the range of forces used. During this experiment, we further confirmed the repeatability of the transients for a given applied force, but noticed changes in the signal as a function of the force applied.

RESULTS

soil-structure interaction

The transients permit us to determine the characteristic coupling resonance of the sensor package and of the main package at this site, where the shear modulus (1-2 dynes/cm^2 in the upper 1 m) and density (1.36 gm/cm^3) of the sediments has been measured independently (Trehu, 1985a). Results of transients on the deployed and main instrument packages are shown in figure 3 in both the time and frequency domains. All three components from a given transient are shown, with the same amplitude scale factor, in order to evaluate possible cross-coupling.

The vertical transient on the deployed sensor package (record BB5 is shown; see appendix 1 for recording parameters and force applied) shows a fairly good response, with a well damped resonant frequency at about 8 Hz. Minor crosscoupling occurred between the vertical and horizontal motion, as indicated by signals recorded on the horizontals from the vertical transient. This may reflect a slightly off-center location of the solenoid. Also noticeable is a high frequency resonance (about 26 Hz) that seems to be excited by the transient. This probably indicates resonance of some element in the seismometer package. It is also seen on the transverse channel

from a radial transient and should be investigated further. The radial transient (BB35 shown, see appendix 1 for parameters) on the sensor package shows a low frequency resonance at about 3 Hz, with a secondary peak at 7 Hz. All transients recorded from the transverse pull (BB30 shown, see appendix 1 for parameters) were clipped, perhaps reflecting human error when adjusting gains.

The transients on the main package are also shown (records BB61, BB23, BB40 are shown; see appendix A for parameters). The vertical transient excites a strong resonance at about 3 Hz. The horizontal resonances also have peaks at about 3 Hz, but are more strongly damped than the vertical resonance. Little cross-coupling is observed.

The resonant frequencies and damping predicted for the recording and sensor packages are compared to the observed resonant frequencies and damping in table 1. The model overestimates both the resonant frequency and the damping for both the sensor and recording packages. We note that these predictions are only crude estimates because of numerous uncertainties. One of the largest uncertainties is the calculation of the hydrodynamic effect on the mass of the recording package. The true effect is certainly quite complicated because of the complicated configuration of the package. We have made two different approximations which probably bracket the actual affect (table 1). Another uncertainty is the shear modulus of the the sediment. Although the shear modulus of the upper meter of sediment has been measured at this site (Trehu, 1985a), the relevant shear modulus is probably an average over some unknown depth, and the proper averaging depth is probably significantly greater for the recording package because of its great mass and larger footprint. The observed damping is probably overestimated because the half-space assumption of the model is violated. A basement layer comprising glacial till is found at a depth of 5 m beneath the experiment site, and seismic energy is probably reflected back into the system by this layer, decreasing the effective damping (Luco, 1976). Contributing to the undertainty in the response of the sensor package is the limited number of transient test conducted. Given these uncertainties, the observations are generally consistent, to first order, with the simple mass-spring-dashpot model. Because of the problems with data quality discussed above, we did not attempt a more sophisticated analysis of the soil-structure interaction (Garmany, 1984).

reradiation of seismic energy

Figure 4 displays composite record sections (using data from BB8, BB10, BB40, BB44, BB49, BB50, BB58, and BB59) showing the signal recorded on the sensor package from transients applied to the main package as a function of the offset between the main package and the sensor package. All three components in the sensor package are shown from transverse transients (A) and from vertical transients (B) on the main package. Clearly a signal is observed on the

sensor package resulting from motion of the main package. The signal is much stronger for transverse motions of the main package than for vertical motions of the main package. In fact, the signal recorded on the sensor package is as large or larger than the signal recorded on the recording package for transverse transients applied to the recording package. This is shown in figure 5, where the transverse signal on the sensor and recording package are compared for a moderate (5.3 kg of buoyancy) and a large (11.7 kg of buoyancy) transient . For both of these examples, the sensor package was located 1 m from the recording package, which represents the offset for a normal field deployment. Spectra of the signals are also shown, and indicate that less 1 Hz energy is observed on the sensor package (containing 1 Hz geophones) than on the main recording package (containing 2 Hz geophones). This is rather surprizing and should be investigated further. The amplitude of the signal recorded in the sensor package resulting from vertical transients on the recording package is much smaller than the signal recorded for horizontal transients, and is not noticeable at all in the data recorded from "small" (2.7 kg of buoyancy) transient, in spite of the fact that a significant coupling resonance is observed on the sensor package.

It is difficult to determine the velocity with which the seismic signal radiated from the main recording package is propagating because of the emergent nature of the signal; uncertainty in the sensor-recorder offset may also contribute. A velocity of about 40 m/s is roughly consistent with the data, as shown in figure 4; this velocity is consistent with seismic shear wave velocities in very low strength sediments. We note that the recorded seismograms are in the near-field since the wavelength of the dominant energy is about 10m. Consequently, the wavefield cannot be separated into distinct P and S waves. Because of the possible distortion of the data resulting from the problems in the recording system, we did not attempt a more sophisticated analysis of the mode of propagation of this energy. None-the-less, we can conclude that significant energy is radiated from the recording package in response to horizontal motions of the recording package. In the field, this effect will probably result in increased seismic noise if the recording package is disturbed by seafloor currents or biological activity. The amplitude of this signal attenuates rapidly with distance, suggesting that an improved response can be achieved by increasing the separation between the recording package and the sensors. This effect is much less severe for vertical disturbances of the recording package.

In order to test the effects of seafloor currents, we had planned to deploy two recording packages near a bottom current meter for several days at a site where strong variations in tidal currents were expected. Four 3-component sensor packages were planned: one package representing the normal configuration of the ONR OBS; a second package measuring motion of the recording package; a third package with the same configuration as the deployed sensor package but

placed about 4 meters feet from the recording package; and a fourth buried and approximately neutrally buoyant sensor package placed about 4 meters from any other packages to provide a control on true ground motion. With this experiment, we had hoped to separate the effects of radiation of energy from the recording package in response to current-induced motions of the main package from effects due to currents on the sensor package itself. We were unable to conduct this part of the experiment when the main stage of field work was conducted because the instruments were not ready for remote, unattended operation. This part of the experiment was rescheduled several times and postponed because of delays in instrument development.

REFERENCES

Arnold, R.M., G.N. Bycroft, and G.B. Warburton, 1955, Forced vibrations of a disc on an infinite elastic body, *J. Appl. Mech. Trans ASME*, v. 77, 391-401

Bycroft, G.N., 1956, Forced vibrations of a rigid circular plate on a semi-infinite elastic space and on an elastic stratum, *Phil. Trans. Roy. Soc. Lond., Ser. A*, v. 248, 327-368.

Bycroft, G.N., 1978, The effect of soil-structure interaction on seismometer readings, *Bull. Seism. Soc. Am.*, v. 68, 823-843.

Duennebier, F.K., G. Blackinton, and G.H. Sutton, 1981, Current generated noise recorded on ocean bottom seismometers, *Marine Geophys. Res.*, v.5, 109-115.

Duschenes, J.D., T.W. Barash, P.J. Mattaboni, and S.C. Solomon, 1981, On the use of an externally deployed geophone package on an ocean bottom seismometer, *Mar. Geophys. Res., v. 4*, 437-450.

Garmany, J.D., 1984, The recovery of true particle motion from three component ocean bottom seismometer data, *J. Geophys. Res.*, v. 89, 9245-9252.

Hsieh, T.K., 1962, Foundation vibrations, *Proc. Institution of Civil Engineers*, v. 22, 211-226.

Iguchi, M. and J.E. Luco, 1982, Vibration of flexible plate on viscoelastic medium, *J. Eng. Mechanics Div. ASCE*, v. 108, 1103-1120.

Jacobson, R.S., L.M. Dorman, G.M. Purdy, A. Schultz, and S.C. Solomon, 1991, Ocean bottom seismometer facilities available, *EOS, Trans. Am. Geophys. Un., v. 72*, pp. 506 and 515.

Jennings, P.C., 1970, Distant motions from a building vibration test, *Bull. Seis. Soc. Am.*, v. 60, 2037-2044.

Kasahara, J., S. Nagumo, S. Koresawa, T. Daikuhara, and H. Miyata, 1980, Experimental results of vortex generation around ocean bottom seismograph due to bottom current, *Bull. Earthquake Res. Inst., Tokyo Univ.*, v. 56, 169-182.

Lamer, A., 1969, Couplage sol-geophone, *Geophys. Prosp.*, v. 18, 300-319.

Luco, J.E., 1974, Impedance functions for a rigid foundation on a layered medium, *Nuclear Eng. Design*, v. 31, 204-217.

Luco, J.E., 1976, Vibrations of a rigid disk on a layered viscoelastic medium, *Nuclear Eng. Design*, v. 36, 325-340.

Luco, J.E. and R.A. Westman, 1971, Dynamic response of circular footings, *J. Eng. Mechanics Div. ASCE*, v. 97, 1381-1395.

Lysmer, J. and F.D. Richart, 1966, Dynamic response of footings to vertical loading, *J. Soil Mechanics and Foundations Div. ASCE*, v. 92, 65-91.

Richart, F.E., Jr., J.R. Hall, Jr., and R.P. Woods, 1970, *Vibrations of Soils and Foundation*, Prentice-Hall, Inc., Englewood Cliffs, New Jersey, 414 pp.

Robertson, I.A., 1966, Forced vertical vibration of a rigid circular disk on a semiinfinite elastic solid, *Proc. Cambridge Phil. Soc. 62 Ser. A*, 547-553.

Safar, M.H., 1978, On the elimination of distrotion caused by the geophone-ground coupling, *Geophysical Prospecting*, v. 26, 538-549.

Sauter, A.W., J. Hallinan, R. Currier, T. Barash, B. Wooding, A. Schultz, and L.M. Dorman, 1990, A new ocean bottom seismometer, in *Proceedings of Conference: Marine Instrumentation '90*, Marine Technology Society, pp. 99-104.

Sutton, G.H., F.K. Duennebier, and B. Iwatake, 1981, Coupling of ocean bottom seismometers to soft bottoms, *Marine Geophys. Res.*, v. 5, 35-51.

Sutton, G.H. and F.K. Duennebier, 1988, Optimum design of ocean bottom seismometers, *Marine Geophys. Res.*

Tréhu, A.M. and S.C. Solomon, 1981, Coupling parameters of the MIT OBS at two nearshore sites, *Marine Geophys. Res.*, v. 5, 69-78.

Tréhu, A.M., 1985a, Coupling of ocean bottom seismometers to sediment: results of tests with the U.S. Geological Survey ocean bottom seismometer, *Bull. Seism. Soc. Am.*, v. 75, 271-289.

Tréhu, A.M., 1985b, A note on the effect of bottom currents on an ocean bottom seismometer, *Bull. Seism. Soc. Am.*, v. 75, 1195-1204.

Wolf, A., 1944, The equation of motion of a geophone on the surface of an elastic earth, *Geophysics*, v. 9, 29-35.

Zelikovitz, S.J. and W.A. Prothero, Jr., 1981, The vertical response of an ocean bottom seismometer: analysis of the Lopez Island vertical transient tests, *Marine Geophys. Res.*, v. 5, 53-67.

TABLE 1: Observed and calculated soil-structure resonances for the ONR OBS

	Sensor package	Recording package
Mass	43 kg	694 kg
Mass corrected for hydrodynamic effects [1]	58 kg	764-1569 kg
Radius [2]	0.20 m	0.48 m
Predicted resonant frequency [3]	15 Hz	4.8-15 Hz
Predicted damping	0.5	0.38-0.54
Predicted damped resonant frequency	11 Hz	3.26 - 12 Hz
Observed resonant frequency	8 Hz	3 Hz
Observed damping	0.4	0.2

notes:

[1] Corrected mass of the sensor package was calculated using the expression for a sphere. No correction was applied for the anchor because water does not flow around the anchor. The corrected mass for the recording package was calculated in two ways, which probably represent extreme values. The range of values given in the table represent the values calculated from these two estimates. The lower value is based on the assumption that the hydrodynamic correction is equal to the correction due to each of flotation balls independantly. The higher value is the correction due to a solid prism with the dimensions of the instrument frame.

[2] The radius given for the main package represents the radius of a circle with the same area as the anchor.

[3] The sediment shear modulus and density used for this calculation were 1.5 dynes/cm^2 and 1.67 gm/cm^3, respectively (Trehu, 1985a).

FIGURE CAPTIONS

Figure 1. Plan (top) and side (botom) view of the new ocean bottom seismometer layout. The conventions for referring to components and recorder/sensor separation, and the configuration of the transient tests discussed in this paper are also shown (adapted from Jacobson et al., 1991).

Figure 2. Example of data showing spurious spikes and the effect of despiking with FAC = 10 amd FAC = 5.

Figure 3. Results of transient tests on the sensor and recording packages. All three components of each transient are shown to illustrate crosscoupling. Traces 1, 2,and 3, and 4, 5, and 6 are the vertical, radial, and transverse components on the sensor and recording packages, respectively. For a given transient, all traces have the same amplitude scale as well as the same time scale. The frequency spectrum is shown for each trace.

Figure 4. Record sections showing seismic energy radiated from the recording package as transients are applied to the recording package. Record sections from each component in the sensor package are shown for (A) tranverse transients and (B) vertical transients. All traces have the same amplitude scale.

Figure 5. Transverse component seismograms recorded on the sensor package (top; trace 3) and on the recording package (bottom; trace 6) from a transverse transient on the recording package. Traces from a large (left) and a moderate (right) transient are shown. All traces are scaled to the same amplitude. Frequency spectra of the traces are also shown.

Figure 6. Vertical component seismograms recorded on the sensor package (top; trace 1) and on the recording package (bottom; trace 4) from a vertical transient on the recording package. Traces from a small transient are shown. All traces are scaled to the same amplitude. Frequency spectra of the traces are also shown.

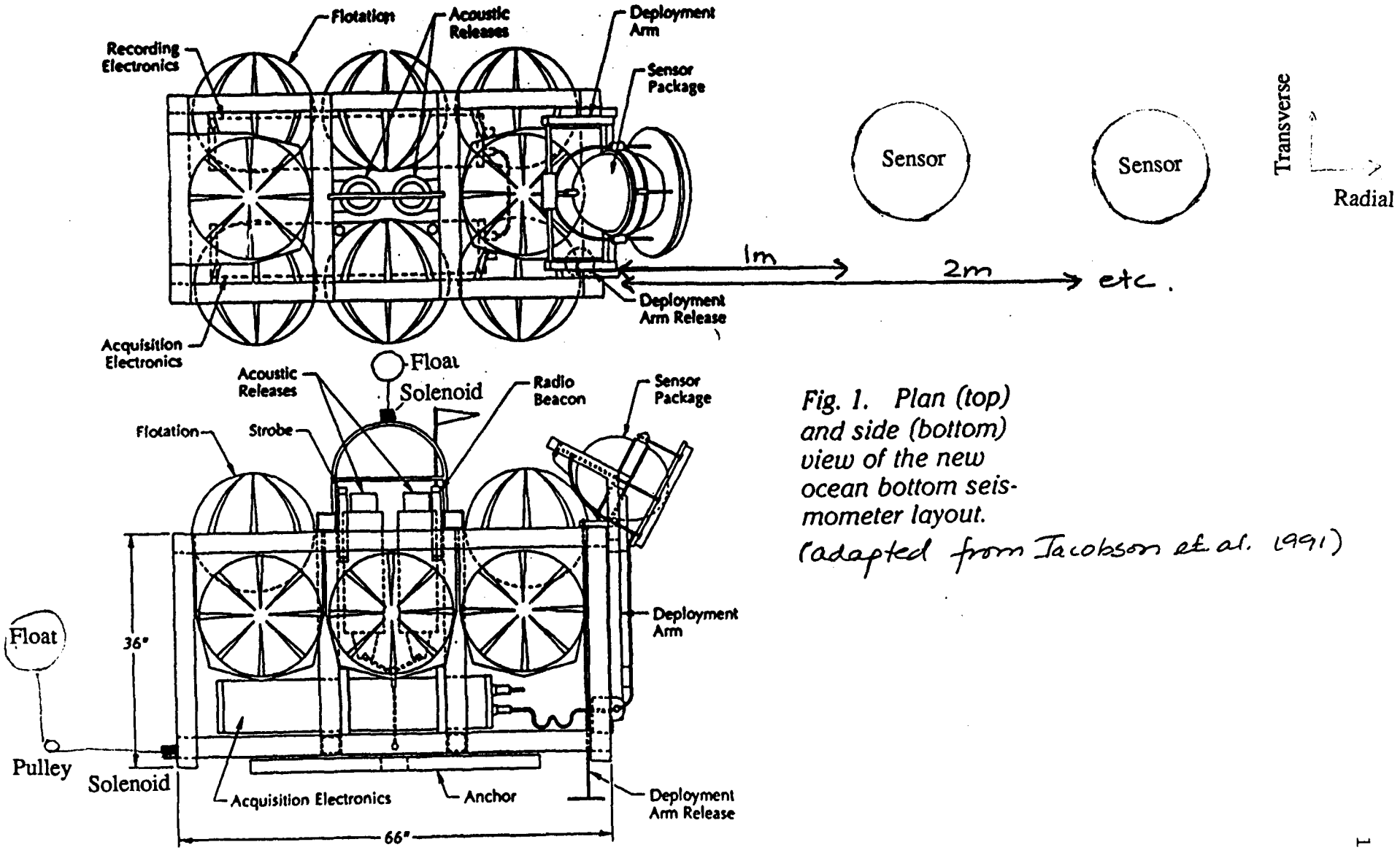

Fig. 1. Plan (top) and side (bottom) view of the new ocean bottom seismometer layout.
(adapted from Jacobson et al. 1991)

figure 1

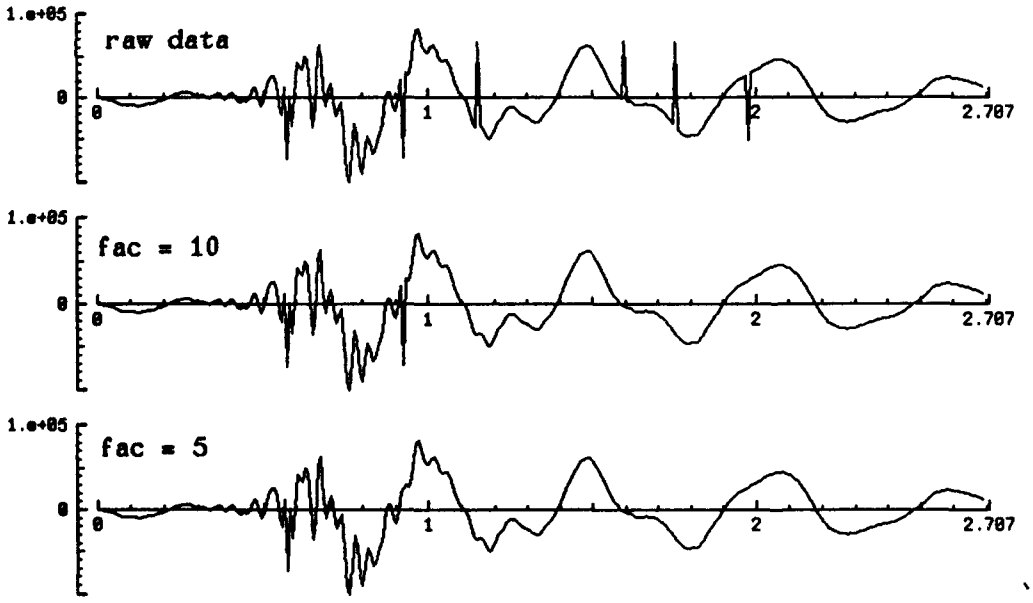
1.e+05
raw data
0
0
1
2
2.707
1.e+05
fac = 10
0
0
1
2
2.707
1.e+05
fac = 5
0
0
1
2
2.707

figure 2.

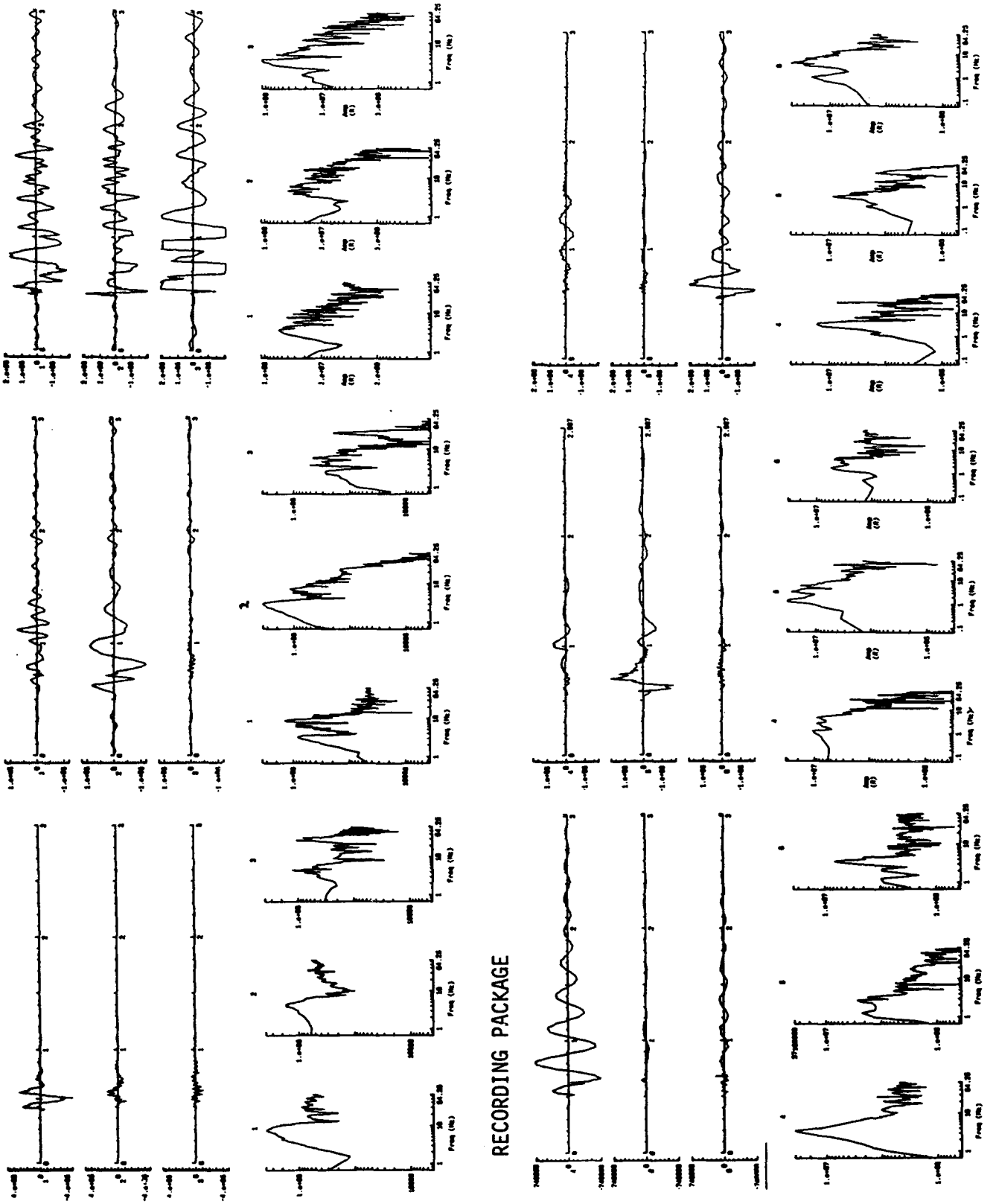

figure 3

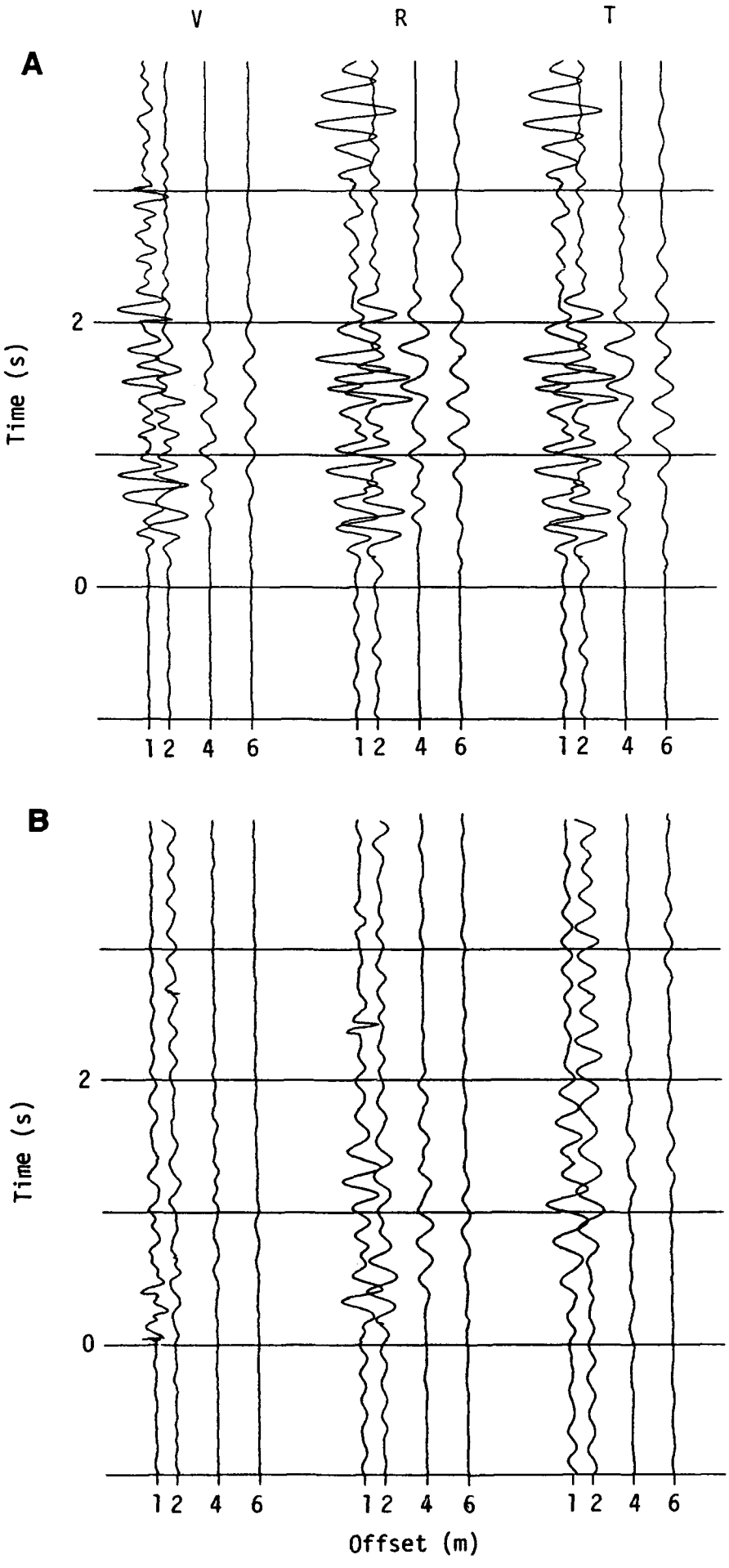

figure 4

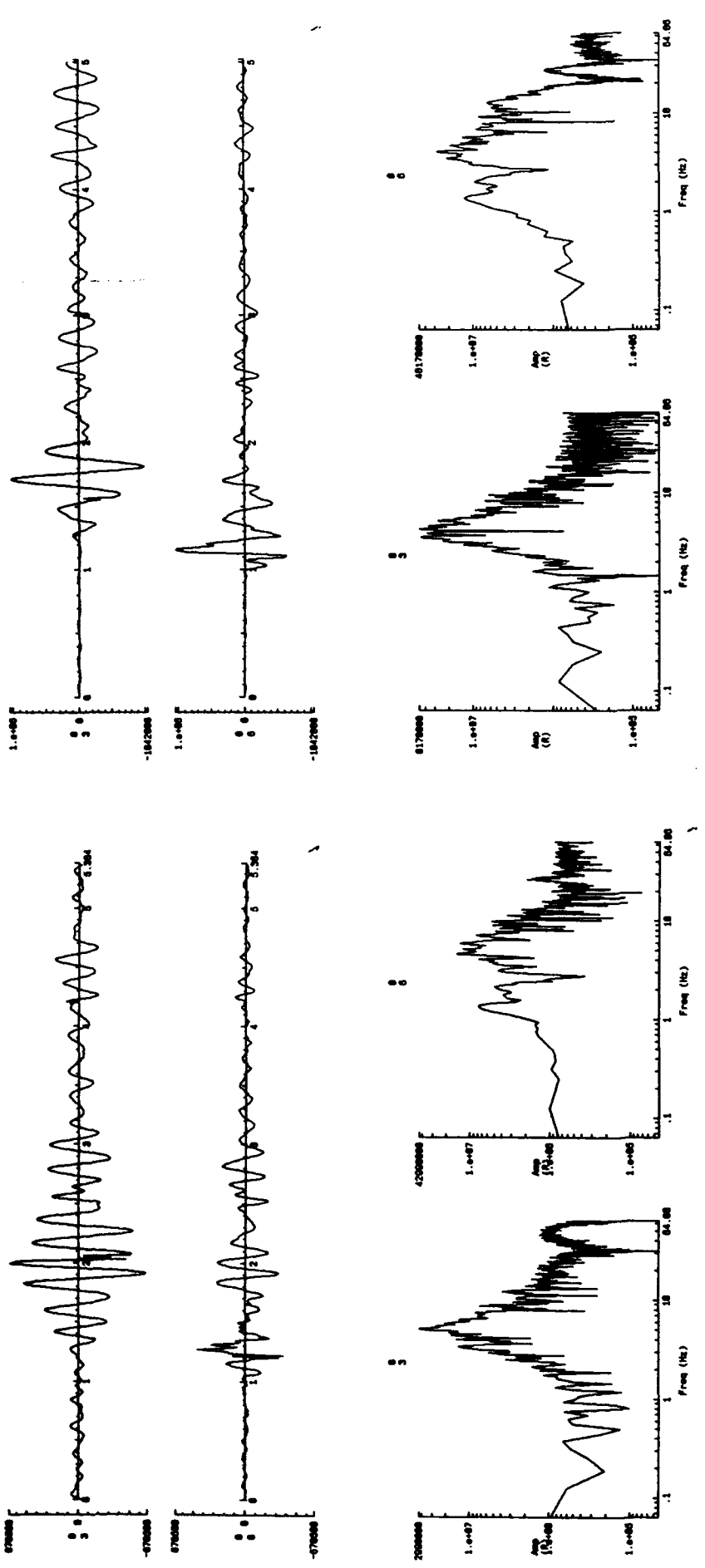

figure 5

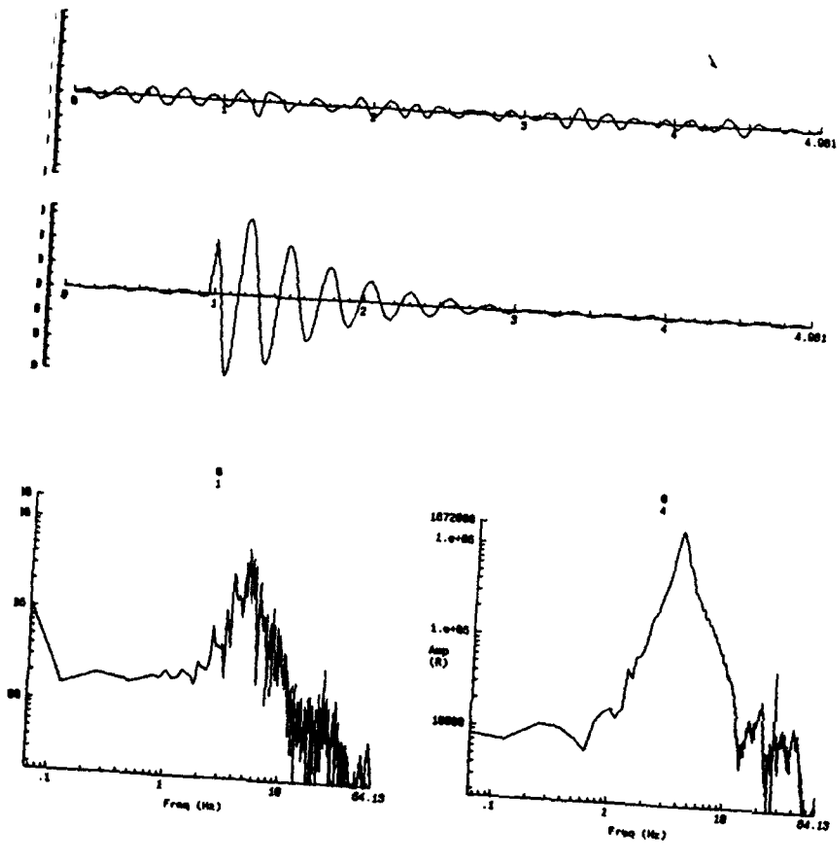

figure 6.

APPENDIX A

SUMMARY OF TRANSIENT TESTS CONDUCTED IN BUZZARDS BAY, NOVEMBER 7-8, 1989

Notation and bouyancy for floats:
yf (yellow float) = 1.82 kg of bouyancy;
of (orange float) = 2.67 kg;
wf (white float) = 3.2 kg.

Gain (g) = 6 unless otherwise specified.

Identification of channels:
Ch1 = 1 Hz vertical geophone in deployed sensor package;
Ch2 = 1 Hz radial geophone in deployed sensor package;
Ch3 = 1 Hz transverse geophone in deployed sensor package;
Ch4 = 2 Hz vertical geophone attached to main recording package;
Ch5 = 2 Hz radial geophone attached to main recording package;
Ch6 = 2 Hz transverse geophone attached to main recording package.

Ten seconds of data were uploaded and 7-8 seconds of data were usable, unless otherwise specified.

BB1: OBS still on deck and engines still on. Test data. g=5
BB2: same as above except g=6

deploy OBS

BB3: Vertical pull on sensor pack w/ 1 yf. g=6. No release.
BB4: same as BB3. Float released. Data clipped.
BB5: same as BB4 except g=2.

sensor pack 1m from main pack:

BB6: Vertical pull on main pack w/ 1 of.
BB7: Vertical pull on main pack w/ 2of.
BB8: Vertical pull on main pack w/ 2of+2wf.

sensor pack 2m from main pack:

BB9: Vertical pull on main w/ 2of.
BB10: Vertical pull on main w/ 2of+2wf.
BB11: Vertical pull on main w/ 2of+4wf. funny ring on vert 2Hz.

problem w/ solenoid

BB12: background noise.
BB13: background noise (bad data)
BB14: background noise.
BB15: background noise. 20 second record.

sensor still at 2m from main.

BB16: Radial pull on main pack w/ 1yf. bad release.
BB17: Same as BB16. bad release
BB18: Same as BB16. bad release
BB19: Radial pull on main w/ 2yf.
BB20: Radial pull on main w/ 2yf+2wf.
BB21: Radial pull on main w/ 1of.

move sensor to 1m from main.

BB22: Radial pull on main w/ 1of.
BB23: Radial pull on main w/ 2of.
BB24: Radial pull on main w/ 2of+2wf.

move sensor to 4m from main.

BB25: Radial pull on main w/ 2of+2wf.
BB26: Radial pull on main w/ 2of.
BB27: Radial pull on main w/ 2of.
BB28: Radial pull on main w/ 1of.

end day 1.

BB29: Background noise on bottom with sensor still lashed to main (test record).
BB30: Transverse pull on sensor w/ 1yf. data clipped.
BB31: Transverse pull on sensor w/ 1yf. g=2. data clipped.
BB32: Transverse pull on sensor w/ 1yf. g=0(?). data clipped.
BB33: Radial pull on sensor w/ 1yf. g=0. failed release.
BB34: same as BB33. failed release.
BB35: same as BB33. good release.
BB36: same as BB33. good release.
BB37: Transverse pull on sensor w/ 1yf. g=?
BB38: Transverse pull on sensor w/ yf. g=0.

move sensor 1 m from main.

BB39: Transverse pull on main w/ 1of. g=6. failed release.
BB40: Transverse pull on main w/ 2of.
BB41: Transverse pull on main w/ 1of.

move sensor 2 m from main.

BB42: Transverse pull on main w/ 1 of.
BB43: Transverse pull on main w/ 2of.
BB44: Transverse pull on main w/ 2of+2wf.

move sensor 4 m from main.

BB45: Bad data file
BB46: Transverse pull on main w/ 2of.
BB47: Transverse pull on main w/ 1of. poor release
BB48: Transverse pull on main w/ 2of+2wf.
BB49: Transverse pull on main w/ 2of+2wf.

move sensor 6 m from main.

BB50: Transverse pull on main w/ 2of+2wf.
BB51: Transverse pull on main w/ 2of+2wf.
BB52: Transverse pull on main w/ 2of.
BB53: Transverse pull on main w/ 2of.
BB54: Transverse pull on main w/ 1of.
BB55: Transverse pull on main w/ 1of.
BB56: Vertical pull on main w/ 1of.
BB57: Vertical pull on main w/ 2of.
BB58: Vertical pull on main w/ 2of+2wf.

move sensor to 4 m from main.

BB59: Vertical pull on main w/ 2of+2wf.
BB60: Vertical pull on main w/ 2of.
BB61: Vertical pull on main w/ 2of.

move sensor to 1 m from main.

BB62: Vertical pull on main w/ 1of.

end of day 2.

APPENDIX B

DATA RECORDED DURING TRANSIENT TESTS CONDUCTED IN BUZZARDS BAY, NOVEMBER 7-8, 1989

All data traces are unfiltered and scaled to the maximum amplitude in the trace.

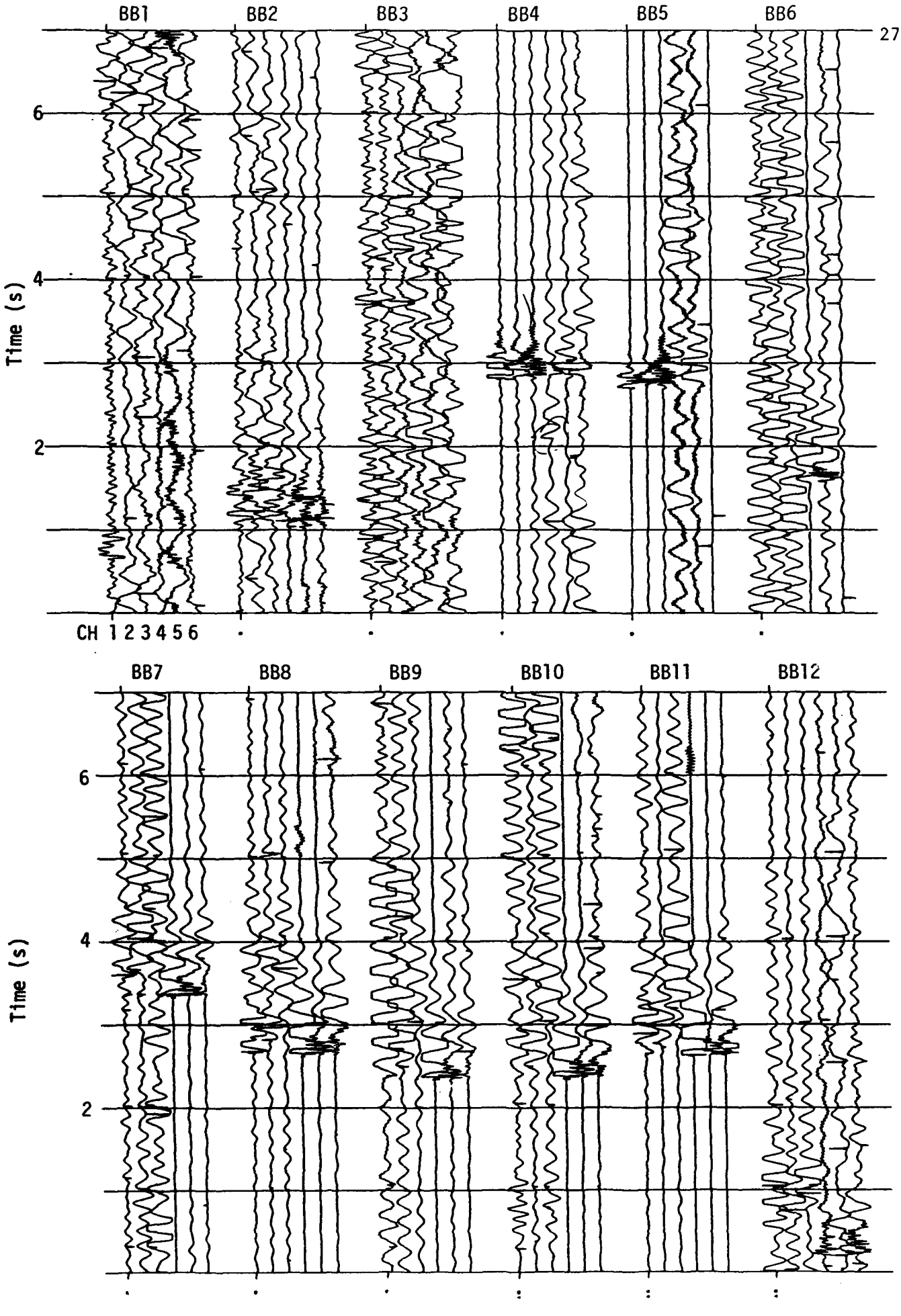
BB1
BB2
BB3
BB4
BB5
BB6
27
6
4
2
Time (s)
CH 1 2 3 4 5 6
BB7
BB8
BB9
BB10
BB11
BB12
6
4
2
Time (s)

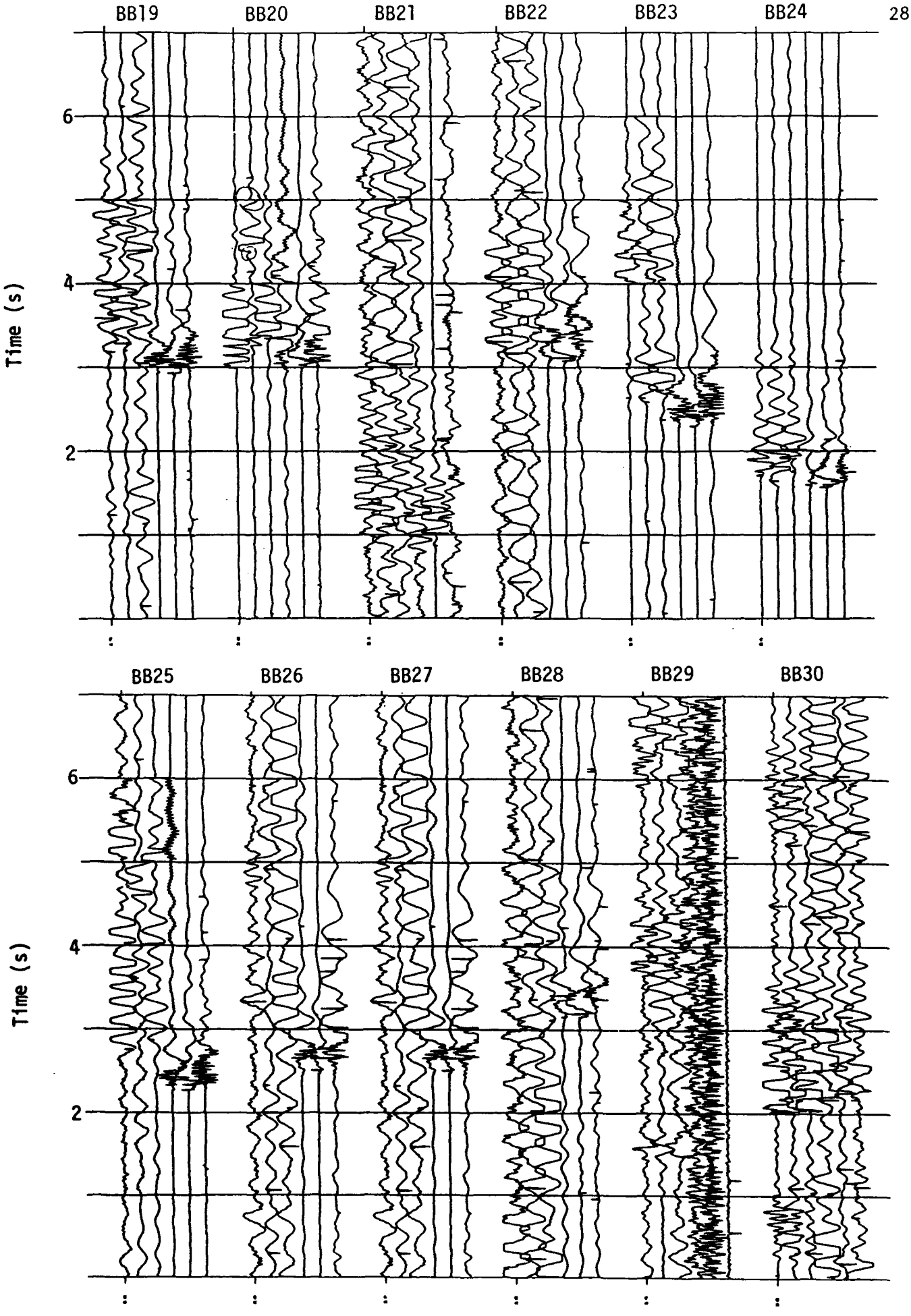
BB19
BB20
BB21
BB22
BB23
BB24
6
4
2
Time (s)
BB25
BB26
BB27
BB28
BB29
BB30
6
4
2
Time (s)

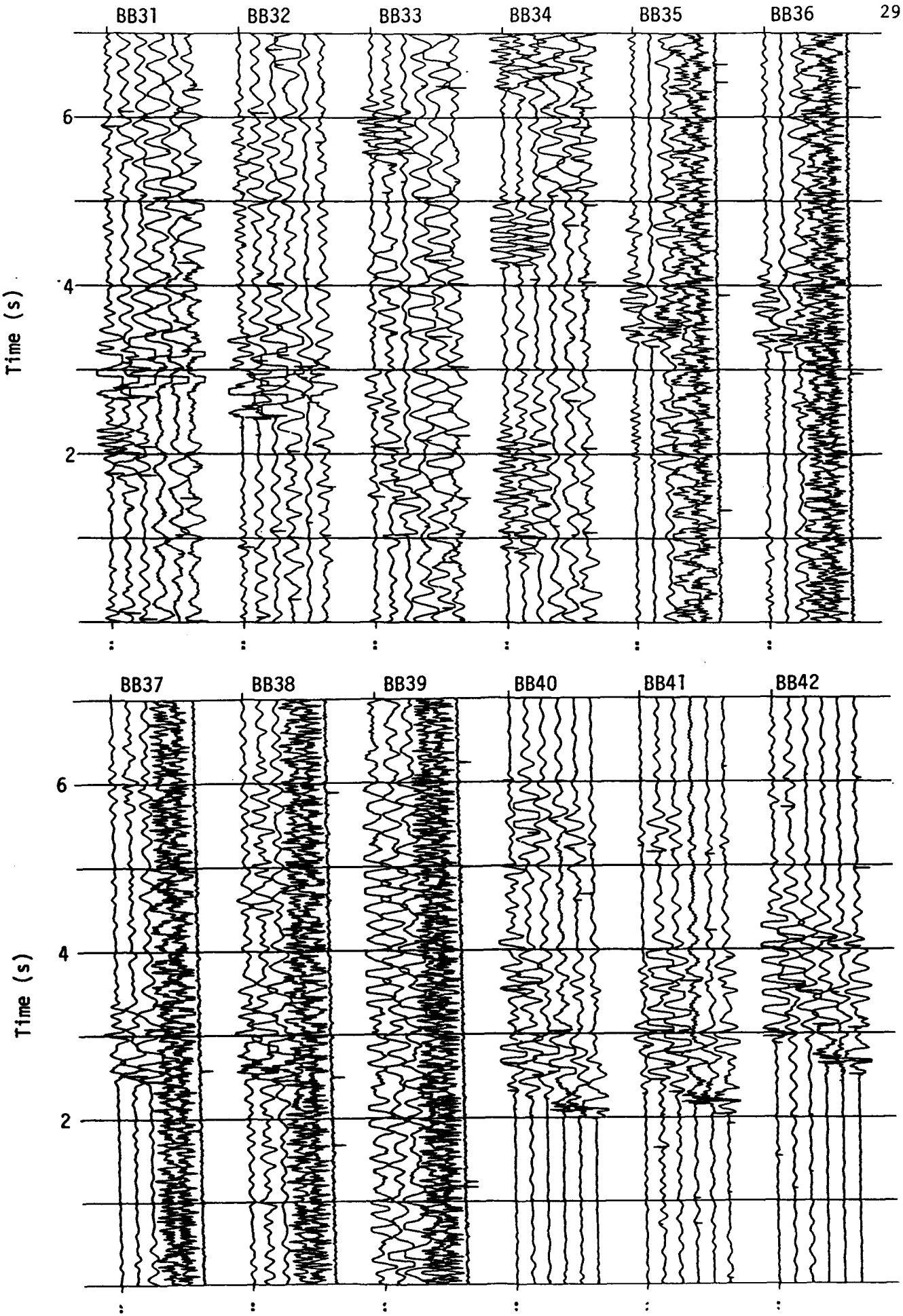
BB31
BB32
BB33
BB34
BB35
BB36
6
4
2
Time (s)
BB37
BB38
BB39
BB40
BB41
BB42
6
4
2
Time (s)

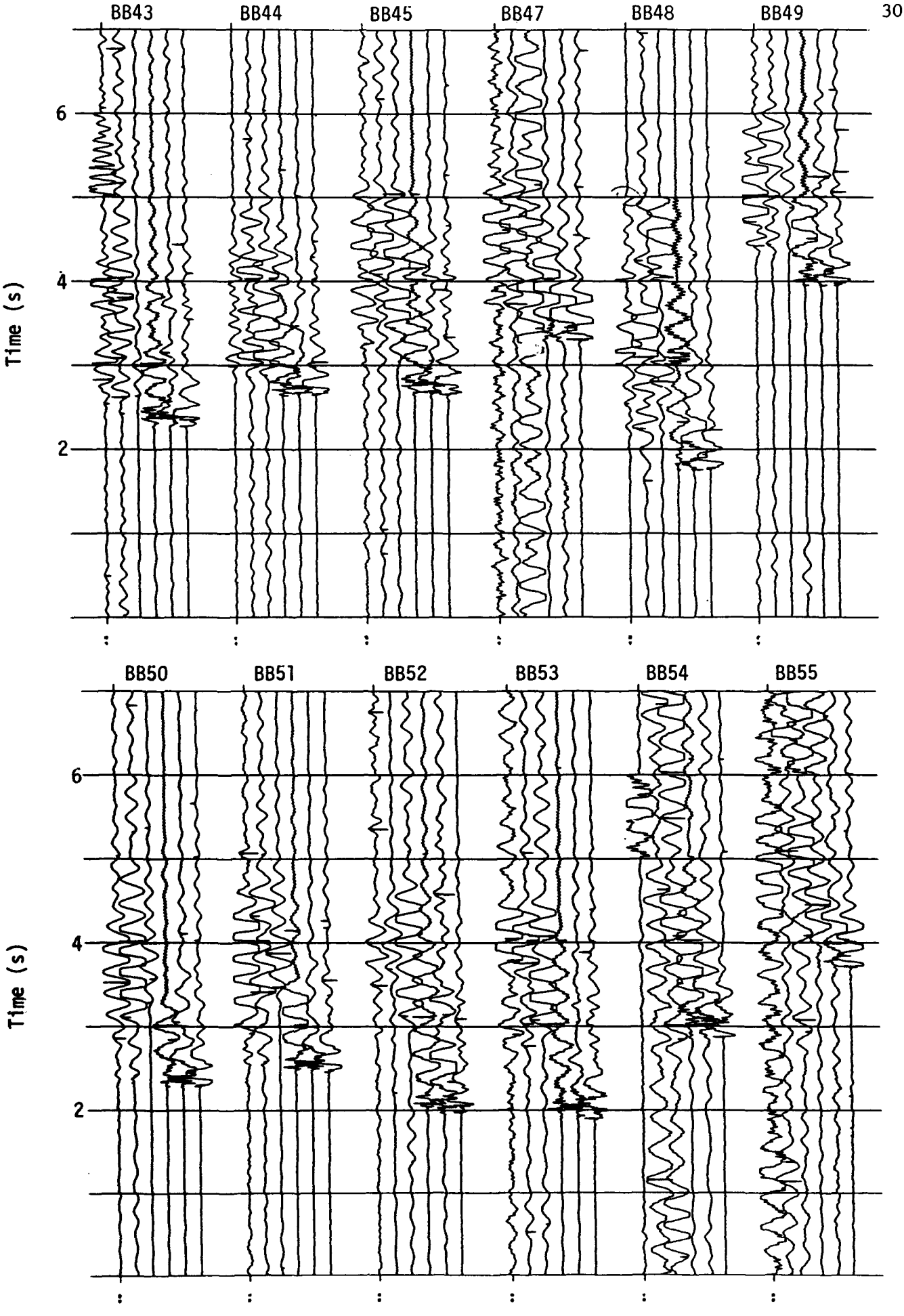
BB43
BB44
BB45
BB47
BB48
BB49
6
4
2
Time (s)
BB50
BB51
BB52
BB53
BB54
BB55
6
4
2
Time (s)

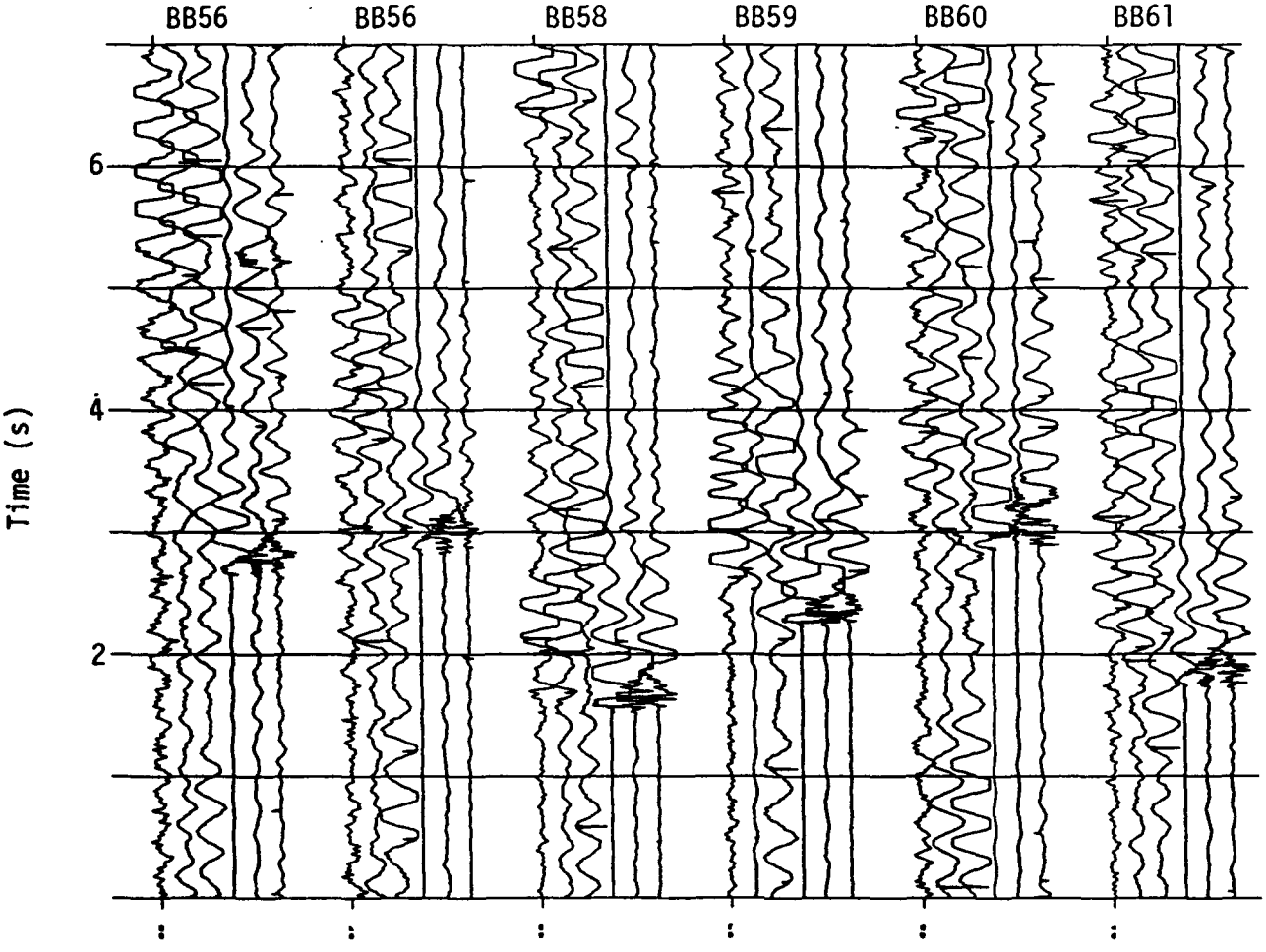
BB56
BB56
BB58
BB59
BB60
BB61
6
4
2
Time (s)

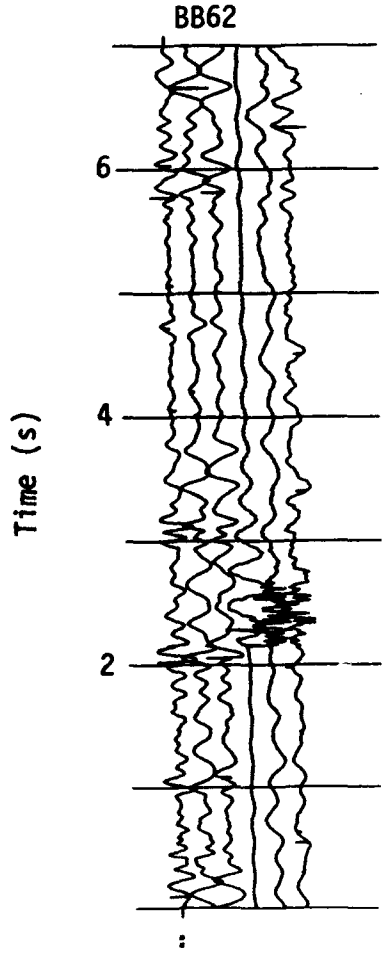
BB62
6
4
2
Time (s)

END

FILMED

DATE: 2-92

DTIC